Mechanical Systems and Signal Processing 147 (2021) 107036

Contents lists available at ScienceDirect

Mechanical Systems and Signal Processing

journal homepage: www.elsevier.com/locate/ymssp

Human-structure dynamic interaction between building floors and walking occupants in vertical direction

Ahmed Mohammed [a,*], Aleksandar Pavic [a]

[a] Vibration Engineering Section, College of Engineering, Mathematics and Physical Sciences, University of Exeter, Exeter EX4 4QF, UK

ARTICLE INFO

Article history:
Received 8 December 2019
Received in revised form 16 April 2020
Accepted 3 June 2020

Keywords:
Vibration serviceability
Human-structure interaction
Floors
Human-induced vibration

ABSTRACT

While modern building floors feature lightweight materials and slender structural elements, their dynamic interaction with walking occupants has not been quantified. This is despite the proven and significant influence of this interaction on human-induced vibration levels of other types of lightweight structures, such as footbridges. This work presents an experimental study to quantify the effect of walking pedestrians on the frequency response functions (FRFs), which are dependant on the corresponding modal properties, of two floors, a relatively light floor with low fundamental frequency and a heavier floor with higher fundamental frequency. It also proposes an improved methodology to take into account the interaction between walking pedestrians and supporting floors in the response calculation of human-induced vibrations. Instead of the conventional mass-spring-damper or inverted-pendulum models, the proposed model utilises two experimentally-driven transfer functions, related to the dynamics of walking individuals, over a range of frequencies between 1 Hz and 10 Hz, to mathematically describe the dynamics of this interaction. Hence, the proposed model is relevant to floors with fundamental frequency less than 10 Hz (i.e. low-frequency floors). The results show that walking occupants can cause significant reduction in the amplitudes of the FRFs. This reduction ranges from 44% and 62% for a floor occupied by two or six walking pedestrians, respectively, to 10% for a heavier floor with a higher fundamental frequency occupied by six walking pedestrians. This implies that ignoring this phenomenon in the design can result in an overestimation of the predicted vibration levels. This is especially the case for floors with relatively low fundamental frequency and modal mass. Furthermore, the derived transfer functions related to the dynamics of walking individuals indicated the existence of three whole-body modes of vibration with frequency less than 10 Hz. The performance of the proposed human-structure interaction model is verified with experimental measurements of vibration responses related to individual occupants walking on three floors. The simulated vibration levels are consistent with their measured counterparts indicating the applicability of the proposed model.

1. Introduction

The new generation of building floors feature more slender structural elements and larger column-free areas than ever before [1,2]. This is due to architectural trends and the recent development of lightweight construction materials and design

* Corresponding author.
E-mail address: asm221@exeter.ac.uk (A. Mohammed).

https://doi.org/10.1016/j.ymssp.2020.107036
0888-3270/

tools. The design of such floors is increasingly governed by vibration serviceability criteria related to human activities, such as walking [3].

These trends in building floor design mean that they are livelier and have lower modal mass than typical older floors. Therefore, their dynamic interaction with walking occupants in the vertical direction is more likely to influence their vibration serviceability performance than previously. Such interaction is not taken into account in any of the current vibration serviceability design guidelines used worldwide and pertinent to building floors [4–9]. This is because, when most of these guidelines were published, more than 10 years ago, floors were generally heavier and stiffer than modern floors, and therefore, human-structure interaction (HSI) did not have a significant influence on their dynamic performance. However, neglecting HSI for modern floors could result in a significant overestimation of human-induced vibrations.

Currently available HSI models are related to pedestrians walking on footbridges. The majority of them are based on modelling the walking individual as either an inverted pendulum (IP) [10,11] or a mass-spring-damper (MSD) [12–15]. IP models are generally complex to implement in the design and have limited robustness [16]. MSD models are more common and easier to use. Their corresponding single-degree-of-freedom (SDOF) natural frequency, 2–4 Hz, is close to the fundamental frequency of a typical footbridge, and therefore, they are proven to be useful and reliable in the design of such structures for vibration serviceability. However, their natural frequency is considerably lower than the fundamental frequency of building floors (typically higher than 4–5 Hz). While the existence of higher order human whole-body mode of vibration for walking individuals, as well as for standing individuals, was reported in the literature [15], reliable quantification of its parameters is a difficult process and is generally missing. Consequently, there is a need for a revised approach to model HSI between walking individuals and supporting floors, taking into account the whole-body dynamics of walking individuals in frequency ranges relevant to dominant modes of vibration for building floors. Such a model currently does not exist in the literature. Therefore, this paper addresses this problem by:

- Quantifying the influence of HSI between single or multiple walking pedestrians and supporting floors, and
- Proposing a HSI model for individuals walking on floors with a fundamental frequency below 10 Hz.

Two floors were tested when they were empty and occupied by single or multiple walking occupants. The influence of the walking occupants on the frequency response function (FRF) magnitude is quantified. The proposed HSI model considers whole-body dynamics of walking individuals for frequency range 1–10 Hz where the fundamental frequency of most floors lies. Hence, the proposed model is relevant to floors with fundamental frequency less than 10 Hz (i.e. low-frequency floors). It is represented by two functions describing the transmissibility of structural acceleration to the human body and the corresponding interaction force applied on the floor. The functions were derived from two separate sets of experimental measurements available in the literature [17,18]. The measurements involve individual test subjects (TSs) instrumented with sensors and walking on an instrumented treadmill or standing on an instrumented force plate shaking in the vertical direction, to study their whole-body dynamics. These measurements (Section 3.2 and Section 3.3) were only used for the model development. The performance of the proposed HSI model is verified by comparing *simulated* human-induced structural vibration using the proposed HSI model with corresponding *measurements*, conducted by the authors, of individuals walking on the two floors.

Section 2 in this paper quantifies the effect of HSI on the FRF of two floors before proposing a methodology to model this phenomenon in Section 3. Section 4 validates the proposed model, while Section 5 presents a parametric study regarding the influence of dynamic properties of the structure on HSI. Finally, Section 6 presents the concluding remarks.

2. Influence of HSI on the FRFs of floors

It has been widely reported that the influence of HSI on human-induced vibration of structures is equivalent to the modification of dynamic properties of the supporting structure, namely, natural frequencies and damping ratios [19,16]. This can be referred to as 'passive' HSI effect, as it does not involve changing the walking behaviour of the occupant. 'Active' HSI effect refers to self-changing of walking behaviour due to the vibration of the supporting structure (which is reported for pedestrians walking on footbridges) [10,20]. However, here it is assumed that vibration levels of floors are not high enough to change the walking behaviour of the occupants.

The modal properties of a structure are closely related to its FRFs. Hence, this section quantifies the influence of HSI on the FRF magnitude of two floors. This was done by conducting a modal testing on the two floors to identify the modal properties of their dominant modes of vibration. This is followed by measuring the magnitude of the FRFs at specific test points (TPs) of the floors when they were empty and occupied by single or multiple walking occupants. The FRFs corresponding to empty and occupied structures were compared, and relevant discussion about the results is provided at the end of this section.

2.1. Modal testing

Modal testing was conducted to measure the FRFs which are used to estimate natural frequency, mode shape, damping ratio and modal mass corresponding to modes of vibration of interest for the two structures explained in this study. Multi-input multi-output (MIMO) modal testing was conducted where multiple APS400 [21] and APS113 [22] electrodynamic

shakers were used to apply uncorrelated random forces on the floor structure. Their input force was calculated by multiplying the acceleration of the moving armature, measured using an Endevco 7754A-1000 piezoelectric accelerometer, by its mass. The corresponding structural response was measured by Honeywell QA750 accelerometers placed on specific TPs in the vertical direction.

The floor input force and output acceleration signals were processed using Data Physics Spectrum Analyser DP730 to calculate the FRFs [23]. A Hanning window with a 75% overlap was used for this purpose. Curve fitting of the calculated FRFs was carried out using ME'scope software [24] to estimate the natural frequency, mode shape, damping ratio and modal mass corresponding to modes of vibration of interest. The software utilises the Rational Fraction Polynomial (RFP) algorithm in the fitting process [25]. The RFP is a multi-degree-of-freedom (MDOF) method that fits an analytical expression to a FRF measurement. The coefficients of the numerator and denominator polynomials are estimated using a minimization process between the measurements and the fitted model. The duration of each test and other test-specific details are explained below.

2.2. Floor A

The laboratory full-scale test floor (Fig. 1) is a reconfigurable structure weighting 15 tonnes located at the University of Exeter and dedicated to research purposes. It comprises Sandwich Plate System (SPS) plates attached to each other, using steel splices, and supported by steel beams. The steel beams are connected to each other using bolts and they are resting on four columns (Fig. 2). The columns are attached to a stiff floor surface using bolts. A detailed description of the structure is available elsewhere [26]. The configuration of the floor, shown in Fig. 1, was not changed or dismantled between different measurements.

2.2.1. FRF measurements of the empty and occupied floor

The test grid corresponding to this floor comprises 21 TPs, as shown in Fig. 3. Two APS400 shakers [21] were placed at TP11 and TP17 (green dots in Fig. 3) and 21 Honeywell QA750 accelerometers were placed at the test grid (Fig. 3). The FRF measurements were conducted when the floor was empty of occupants [27]. The test lasted approximately eight minutes, during which six data blocks, each lasting 80 s, were recorded. The maximum sampling frequency was set to be 80 Hz and the number of spectral lines was 3200 resulting in a frequency resolution of 0.0125 Hz. The mode shapes of the lowest four vertical modes of vibration corresponding to the empty floor are shown in Fig. 4.

A nominally identical measurement of the FRFs, as for the empty floor, was conducted when the floor was occupied by two (TSs 1 and 2), four (TSs 1–4) or six (TSs 1–6) pedestrians walking on Floor A (Fig. 5). The test was conducted once for each group size apart from the test which involved six TSs which was repeated twice to test the repeatability of such measurements, as explained below. Before each test, the occupants were asked to walk continuously in random walking paths on Floor A and avoid colliding with each other during the measurements. The aim of these tests was to study whether walking occupants have an effect on the FRF magnitude of the floor for various walking paths and scenarios, rather than targeting a walking path related to the highest influence of walking occupants on the FRF magnitude.

It is worth mentioning that the input for the FRF measurements was only the shakers' forces (the moving masses of the shakers multiplied by their vertical acceleration) while the footfall loading of the walking occupants was assumed to be a

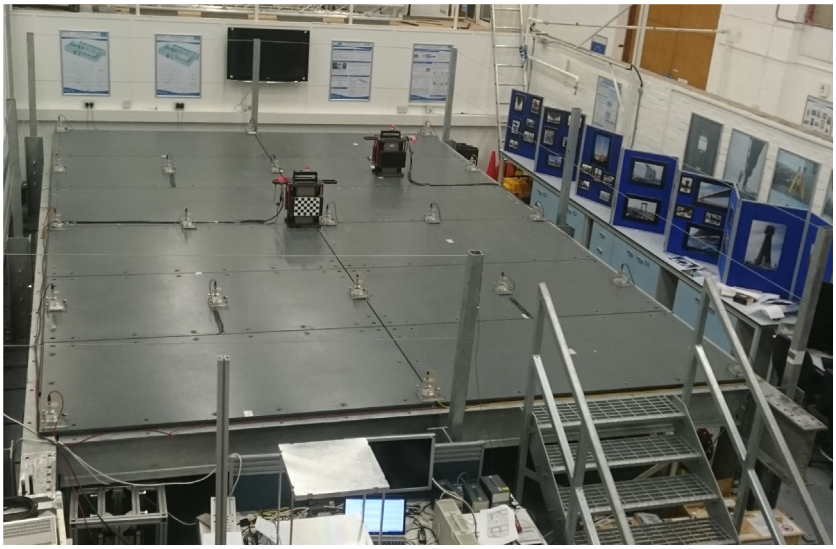

Fig. 1. Overview of Floor A [27].

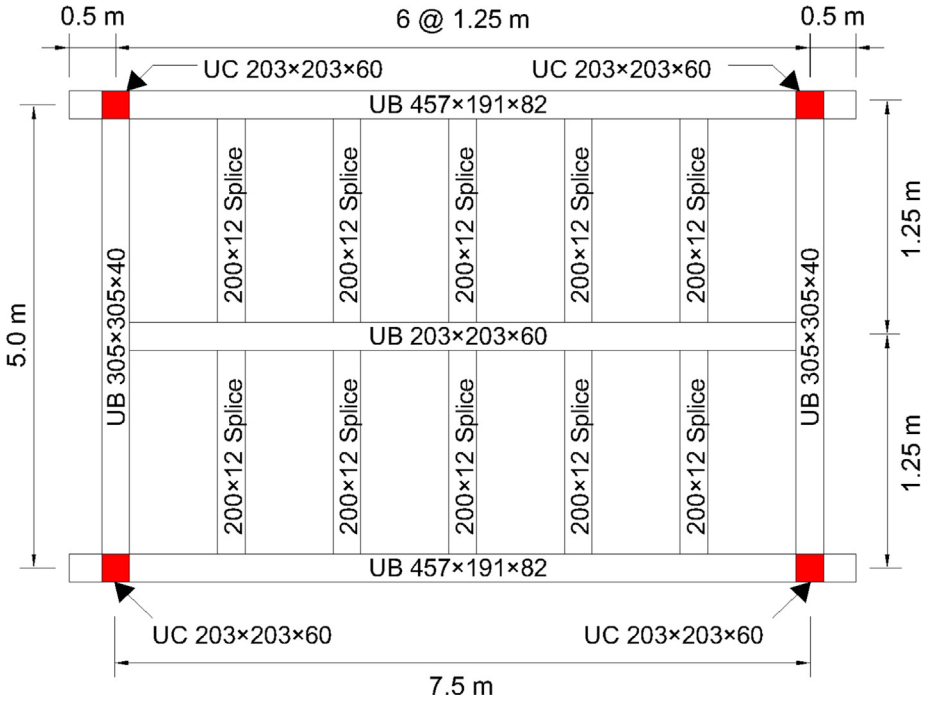

Fig. 2. Key structural elements of Floor A. Red squares represent columns locations. (For interpretation of the references to colour in this figure legend, the reader is referred to the web version of this article.)

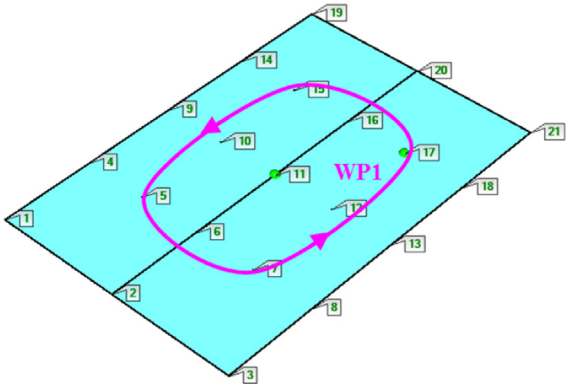

Fig. 3. Test grid used for the FRF measurements of Floor A. Green dots represent shakers locations (TP11 and TP17). (For interpretation of the references to colour in this figure legend, the reader is referred to the web version of this article.)

background noise that can be averaged out throughout the FRF measurements. This also implies that the influence of vibration of the floor caused by footfall loading on the shaker was not taken into account. However, it is believed that such effect is small in comparison with vibration of the floor caused by the shaker forces. This assumption was utilised previously by Zivanovic et al. [28] while conducting similar measurements on a footbridge. The magnitude of the FRFs measured in this study is shown in Fig. 6.

Fig. 6a shows that there was a significant reduction in the FRF magnitude at the fundamental frequency (up to around 50%) even when only two pedestrians were walking on the floor. A slight increase of the fundamental frequency could also be noticed as the number of walking occupants increased (Fig. 6b). Interestingly, the reduction in FRF magnitude at the fundamental frequency was apparently similar when two and four pedestrians were walking on the floor. The reason for this could be explained by the random walking path followed by the walking pedestrians during each test and the corresponding mode shape amplitude for the first mode of vibration (Fig. 4a). In essence, walking close to the edges of the floor could involve less interaction between the walking occupants and the first mode of the floor, but more interaction between the occupants and the second and third modes (Fig. 4).

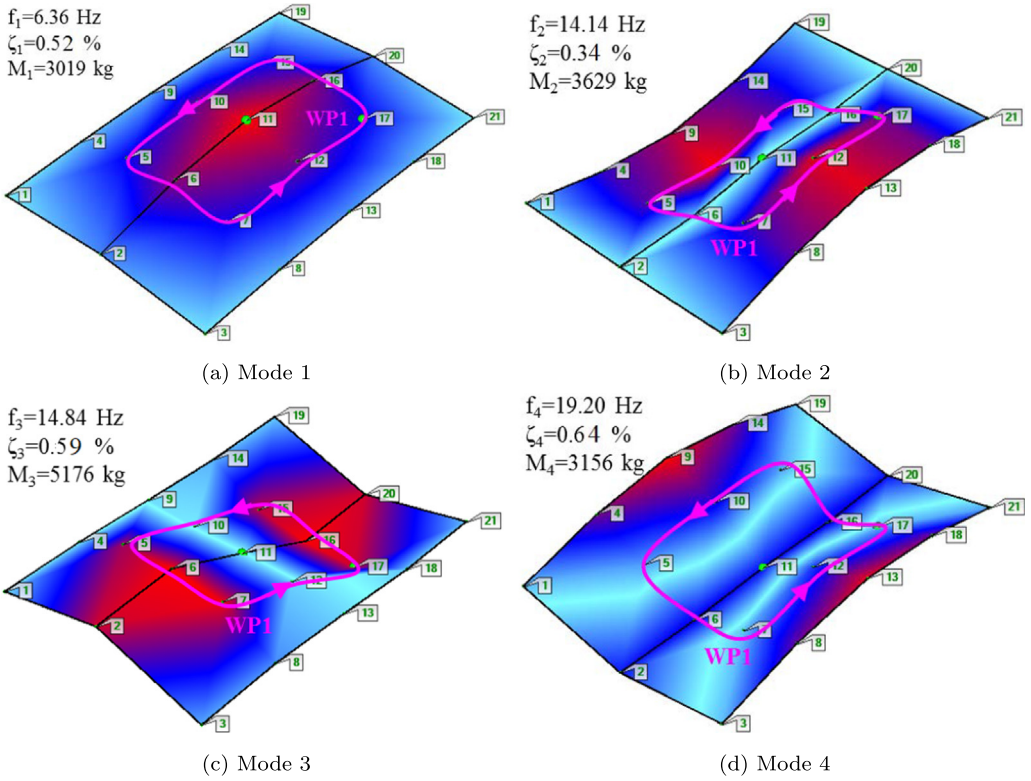

Fig. 4. Mode shapes of the lowest four modes of vibration for Floor A when it was empty from occupants.

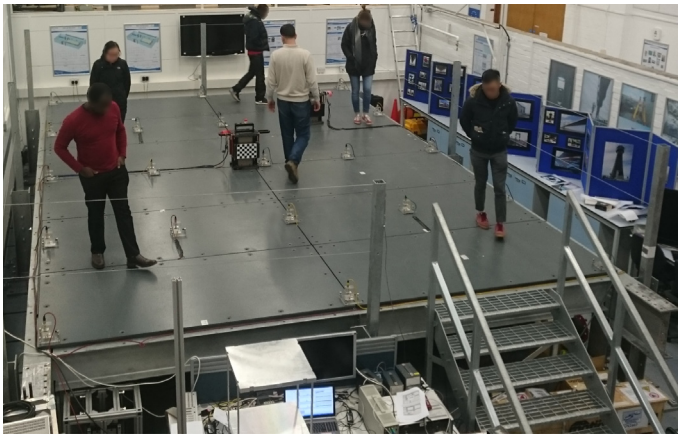

Fig. 5. FRF measurement of Floor A when occupied by six pedestrians [27].

To assess how repeating these tests can affect the measured FRF magnitude, the measurement related to six TSs were repeated twice, and the corresponding results are shown in Fig. 7. Fig. 7 shows that while the FRF magnitude related to the two tests, when six TSs were walking on the floor, are not identical, they are quite similar.

It is worth mentioning that while the mechanical properties of human body may slightly differ between different people, their interaction with the supporting structure may also differ when different people or a combination of people walk on a floor structure. Therefore, the reductions in the FRF magnitude reported in this section may differ if different TSs or a different combination of them walk on the same floor. However, the TSs participated in these tests were chosen randomly, and therefore, it is expected that such a difference may not be significant.

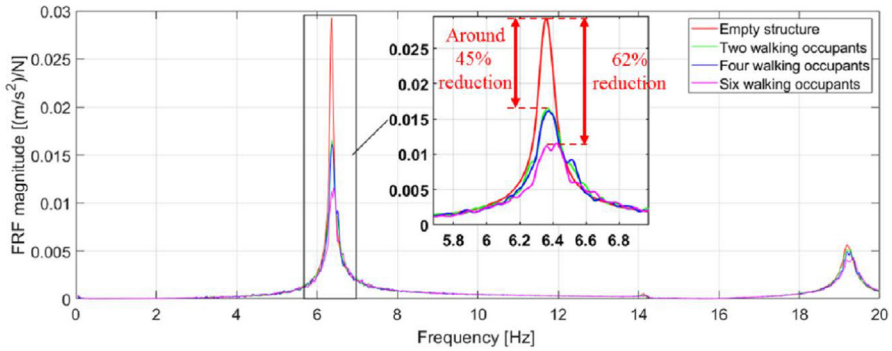

(a) TP11

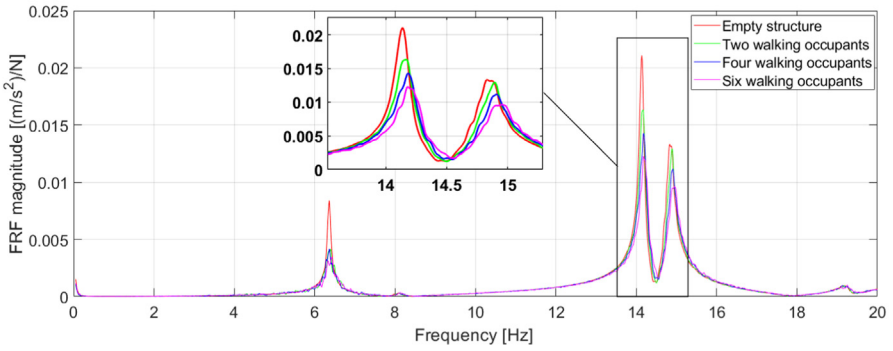

(b) TP17

Fig. 6. FRF magnitude measured at (a) TP11 and (b) TP17 (Fig. 3) on Floor A when it was empty and occupied by walking pedestrians.

2.3. Floor B

The floor (level 1 of the building shown in Fig. 8) is a normal weight steel–concrete composite system, having 130 mm deck thickness, under construction. The floor was tested as a bare structure and before installing façade, raised floors, ceiling panels and other mechanical ducts. As the west and east wings of the first floor are almost identical, only the west wing was tested. Fig. 9 shows the testing area and its corresponding key structural elements.

2.3.1. FRF measurements of the empty and occupied floor

The test grid used for modal testing of Floor B is shown in Fig. 10. Three shakers – two APS400 [21] and one APS113 [22], were placed at TP24, TP42 and TP64, respectively, and 20 Honeywell QA750 accelerometers were used to measure the corresponding structural acceleration at the test grid in five 'swipes' (Fig. 10). The measurements of the FRFs were conducted when the floor was empty. Each test took about ten minutes, during which 20 data blocks, each lasting 40 s, were collected. The maximum frequency was set to be 40 Hz and the number of spectral lines was 3200 resulting in a frequency resolution of 0.025 Hz. The corresponding mode shapes of the lowest four modes of vibration corresponding to an empty floor are shown in Fig. 11.

To measure the FRF corresponding to an empty and an occupied floor, one accelerometer and the three shakers were placed at TP44 (the anti-node of the first, third and fourth modes of vibration). This test set-up was made to maximize the excitation energy applied to these modes. A swept sine excitation with a frequency spanning between 8 Hz and 11 Hz, which covers the range of frequencies of the lowest four modes of vibration (Fig. 11), was used to drive the synchronised shakers with the same signal. Each test lasted about five minutes, during which 10 data blocks, each lasting 40 s, were collected with frequency resolution of 0.025 Hz.

The FRF was measured three times, during which the testing area was empty and occupied by six pedestrians walking in two walking paths (Fig. 12). In the first test (Fig. 12a), the pedestrians were walking along a circular walking path around the shakers (WP1), while in the second test (Fig. 12b) they were walking along WP2 and WP3 in two groups. The reason behind utilising these WPs, rather than random WPs as for Floor A, is that Floor B has higher fundamental frequency and mass than that for Floor A, and therefore, the influence of HSI on FRF magnitude may not be obvious. Hence it was decided to focus on 'extreme' walking scenarios where the occupants were walking close to the antinodes of the dominant modes of vibration to maximise the interaction with these modes. Nevertheless, the focus here was to observe if HSI does have a significant influence on the floor's FRF magnitude rather than to directly compare that with Floor A.

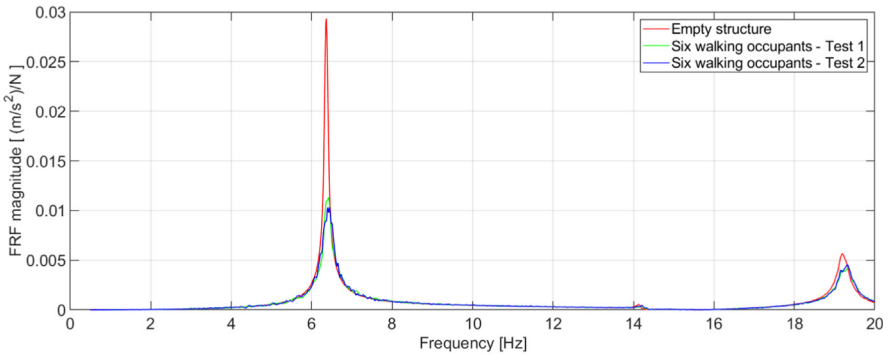

(a) TP11

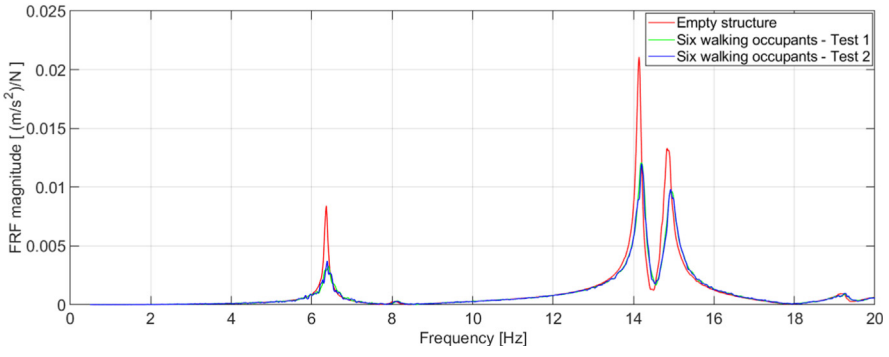

(b) TP17

Fig. 7. FRF magnitude for two nominally identical tests related to six TSs walking on Floor A at (a) TP11 and (b) TP17 (Fig. 3).

Fig. 8. Panoramic view of the building containing Floor B (The far half of the first floor).

Fig. 13 shows the FRF magnitude at TP44 when the testing area was empty and when it was occupied by the walking pedestrians. The reduction in FRF magnitude at the fundamental frequency (9.47 Hz) was approximately 10% and 22% when the pedestrians were walking along WP1 and when they were walking along WP2 and WP3, respectively, compared to that when the testing area was empty.

2.4. Discussion

Table 1 summarises the approximate reductions in FRF magnitudes at the fundamental frequency of the two floors when occupied by walking pedestrians compared to those when the floors were empty. The results summarised in Table 1 show that the influence of HSI on the FRF magnitude of floors varies between different types of floor systems. The highest reduction in FRF magnitude at the fundamental frequency was noticed for Floor A (62%) (Table 1).

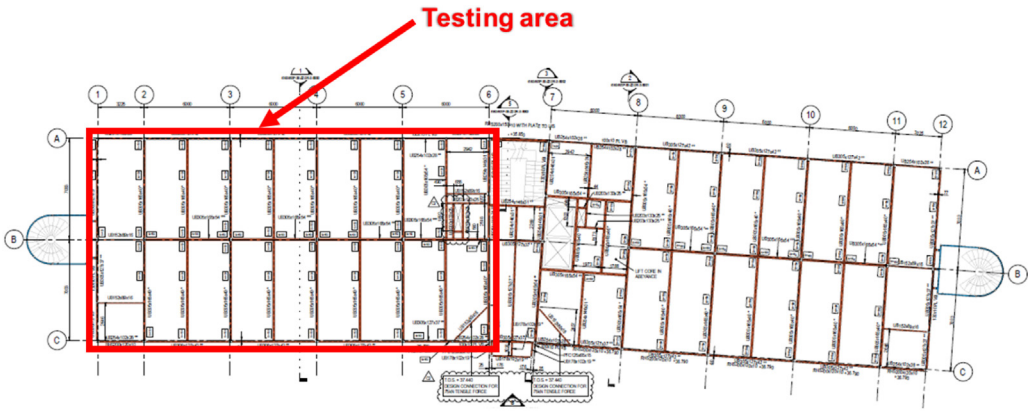

(a) Plan view of the first floor of the building and the testing area.

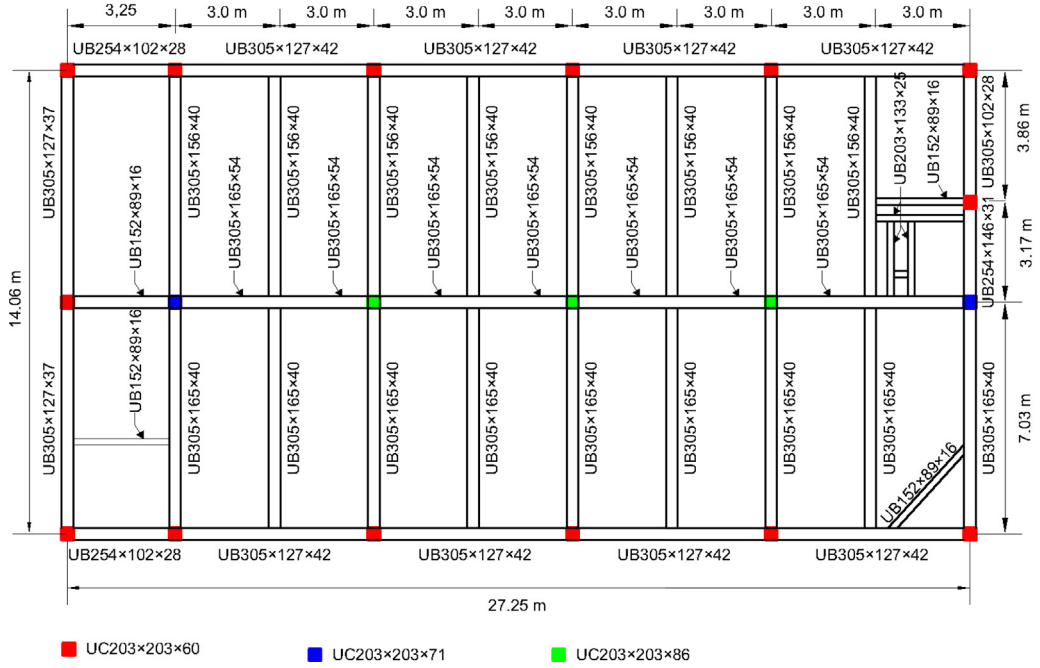

(b) Key structural elements in the testing area of Floor B.

Fig. 9. (a) Testing area of Floor B and (b) the corresponding key structural elements. Red, blue and green squares refer to columns locations. (For interpretation of the references to colour in this figure legend, the reader is referred to the web version of this article.)

Floor B had a limited influence of walking pedestrians on its FRF magnitude at the fundamental frequency despite the fact that the six pedestrians were walking close to its anti-node. This could be related to its relatively high fundamental frequency and modal mass compared to that for Floor A.

Despite having different WPs and number of pedestrians to quantify the effect of HSI on the two floors, certain trends can be observed. It is apparent that the reduction in the FRF magnitude at fundamental frequency is higher for floors with lower natural frequency and modal mass. It is not obvious whether the same trend applies to modal damping ratios as the lowest modes for Floor A and Floor B have similar modal damping ratios. Nevertheless, by curve-fitting the FRFs related to Floor A, it is apparent that the damping ratio related to the first mode was increased from 0.52% for the empty structure to 0.95%, 0.99% and 1.38% when the floor was occupied by two, four or six walking pedestrians, respectively. Hence, a higher reduction in FRF magnitude at the fundamental frequency was also noticed when a higher number of pedestrians were walking on the floor

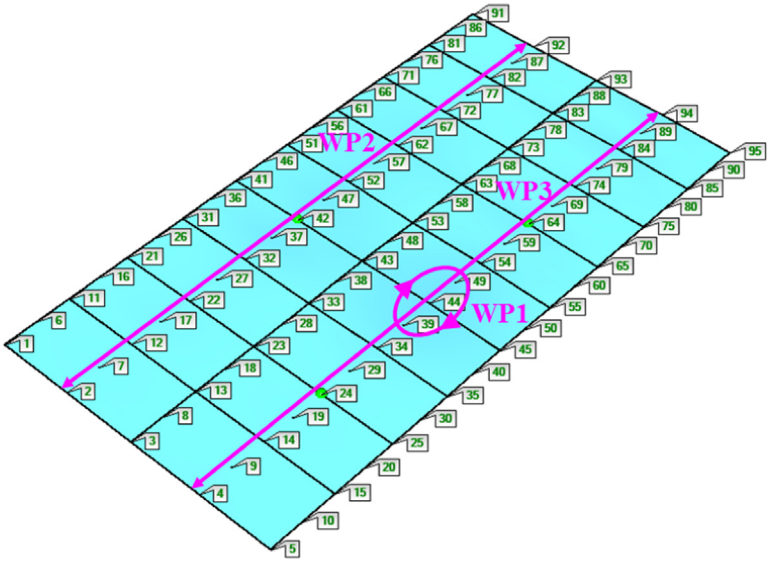

Fig. 10. Test grid used for modal testing of Floor B.

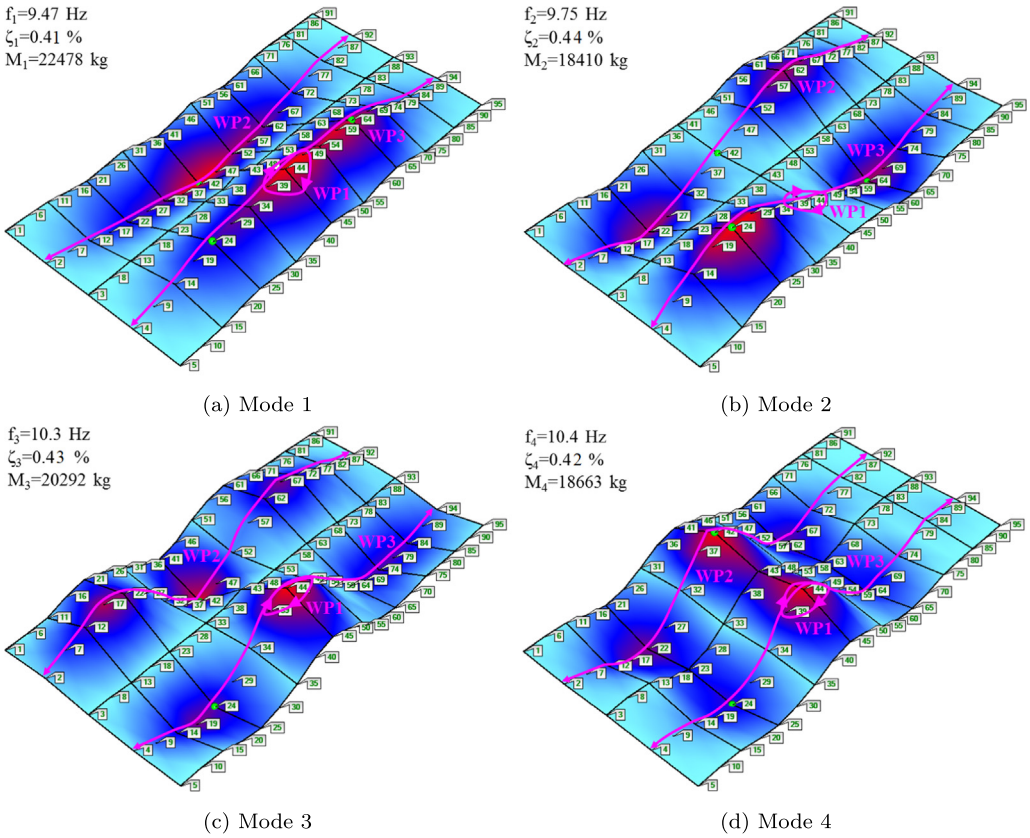

Fig. 11. Mode shapes of the lowest four modes of vibration for Floor B when it was empty from occupants.

(Table 1). The reduction in the FRF magnitude at fundamental frequency for Floor A was 62% when the floor was occupied by six pedestrians, compared to 44% when it was occupied by two pedestrians. Hence, it is apparent that the reduction in the magnitude of the FRFs depends on the modal properties of the floor and the number of walking occupants. This reduction in FRF magnitude can result in a significant reduction in the corresponding human-induced vibration of floors. Therefore, the

(a) Walking in on WP1. (b) Walking across WP2 and WP3.

Fig. 12. FRF measurement of Floor B (at TP44) when occupied by six pedestrians walking (a) on WP1 or (b) along WP2 and WP3 (Fig. 10).

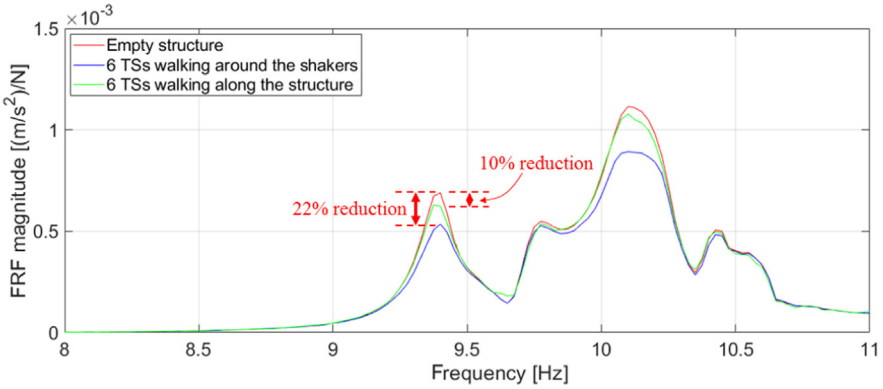

Fig. 13. FRF magnitude at TP44 on Floor B when it was empty and occupied by six walking pedestrians (Fig. 12).

Table 1
Reduction in FRF magnitude at the fundamental frequency of two floors when occupied by walking pedestrians.

Floor	Fundamental frequency [Hz]	No. of pedestrians	Mode of walking	Reduction in FRF magnitude at fundamental frequency [%]
Floor A	6.36	2	Random	44
		4	Random	46
		6	Random	62
Floor B	9.47	6	Along WP1 (Fig. 11a)	22
			Along WP2 and WP3 (Fig. 11a)	10

next section describes a novel methodology to consider HSI in the calculation of footfall-induced vibration specifically of floors.

3. Modelling of HSI between walking occupants and the supporting floors

This section describes an improved methodology to take into account HSI between walking pedestrians and the supporting floors in the vibration response calculations. An overview of the methodology is presented, followed by a description of how it is derived before explaining its implementation.

3.1. Overview

When a pedestrian walks on a flexible floor structure, the corresponding structural acceleration of the vibrating floor can be transmitted to their body which accelerates and applies an interaction force back to the floor (Fig. 14). Hence, if the ground reaction force (GRF) is to be measured for a pedestrian walking on a vibrating surface, then it will include the interaction force and, therefore, such force does not exist for individuals walking on a rigid surface. This 'exchange' of structural

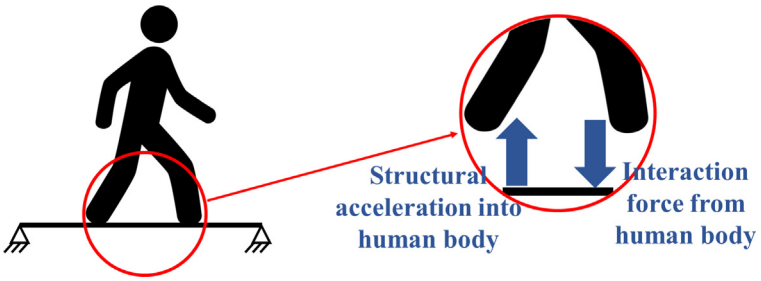

Fig. 14. 'Exchange' of structural acceleration and interaction force between a walking pedestrian and a supporting structure.

acceleration and interaction force between the vibrating floor and a walking occupant form the HSI. Its effect is equivalent to the modification of the modal properties or FRF of the floor, as reported in the literature [18,15]. In essence, the modal properties of the occupied floor can be considered the same as that for an empty floor if structural acceleration and the corresponding interaction force 'exchanged' between the floor and a walking occupant are addressed adequately. This is the basis of the HSI simulation methodology explained in this section.

Previous studies showed that the vertical acceleration of the 7th cervical vertebrae (C7) is well correlated with the corresponding GRF [18,29]. Hence, the proposed HSI methodology assumes that human body mass can be treated as a concentrated mass at the location of C7. The elements of the proposed HSI model are (Fig. 15):

- A single mass representing the mass of a human body,
- The supporting structure,
- A function ($H_{a,a}(f_i)$) to calculate the vertical acceleration of the human body mass transmitted from the vibrating structure, where a (in $H_{a,a}(f_i)$) refers to acceleration of both the input (structural acceleration) and the output (acceleration of human body mass) to $H_{a,a}(f_i)$ and f_i is the frequency of mode i of an empty structure [Hz], and
- A function ($H_{a,F}(f_i)$) to calculate the interaction force from the relative vertical acceleration (a) between human body mass and the structure at the point of contact between them, where F denotes the force as an output of $H_{a,F}(f_i)$. It is assumed that this function can be used to calculate the ground reaction force (related to the desire of the walker to walk on a rigid surface) and the interaction force (related to the acceleration of the supporting surface and, subsequently, the relative acceleration between the walker's body and the supporting surface).

A detailed description of $H_{a,a}(f_i), H_{a,F}(f_i)$ and the implementation of the proposed HSI methodology is presented below. It is worth mentioning that the HSI methodology presented in this section assumes linear behaviour for both human and structural dynamics.

3.2. Acceleration of human body mass

Following the principle of superposition, GRF related to an individual walking on a flexible structure can be treated as a summation of two components (Fig. 16) [14,30]:

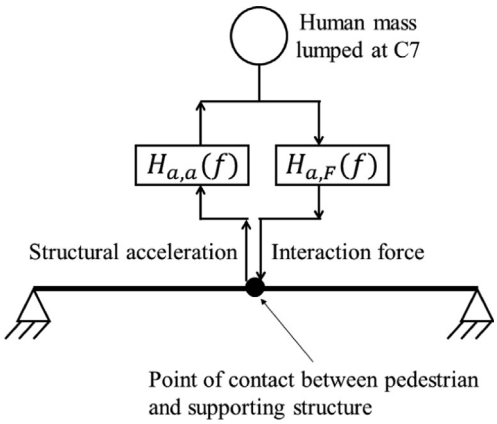

Fig. 15. Components of the proposed HSI model.

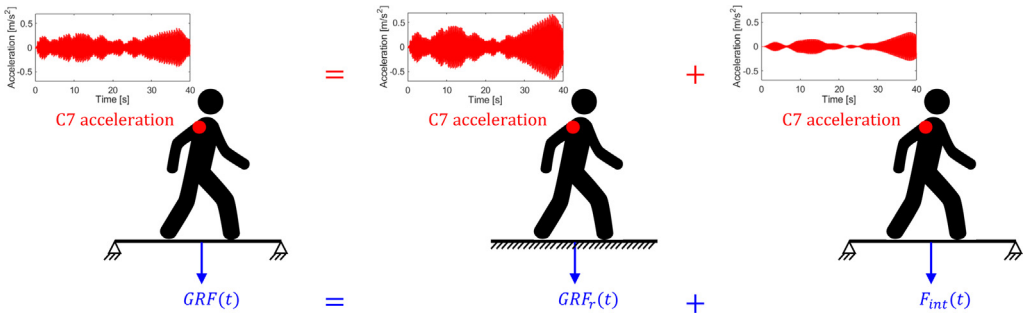

Fig. 16. Schematic representation of C7 acceleration and the corresponding ground reaction force for an individual walking on a flexible structure.

- Ground reaction force component, related to walking on a *rigid* surface ($GRF_r(t)$), where r denotes a rigid surface and t is time, and
- Interaction force between the walking individual and the structure ($F_{int}(t)$), where *int* denotes the interaction term.

Similarly, this study assumes that the acceleration of human body mass has two components:

- Acceleration related to walking on a rigid surface ($GRF_r(t)$) (Fig. 16). It is worth mentioning that humans are sensitive to vibration and they adapt their gait, when walking on a vibrating surface [31]. However this study assumes that vibration levels of floors are not high enough to affect the gait of the occupants significantly. Therefore, it is assumed that the acceleration of human body related to the desire to walk on a vibrating surface is the same as that related to walking on a rigid surface.
- Acceleration caused by vibration of the supporting surface which corresponds to the interaction force ($F_{int}(t)$) (Fig. 16).

The former component of acceleration is implicitly taken into account in $GRF_r(t)$ while the later is calculated as described in the rest of this subsection.

Matsomoto and Griffin [17] measured the transmissibility of vertical acceleration between a vibrating platform and the fourth lumbar vertebrae (L4) for 12 individual test subjects *standing* on it. They described the transmissibility mathematically as in Eq. (1).

$$H_{a,a}(f) = S_{sl}(f)/S_{ss}(f), \tag{1}$$

where, $H_{a,a}(f)$ is the transmissibility at frequency f, $S_{sl}(f)$, in $[(\mathrm{m/s^2})^2/\mathrm{Hz}]$, is the cross spectral density between vertical acceleration of the supporting surface (platform) and vertical acceleration of L4, where, s and l denote the supporting surface and L4, respectively. $S_{ss}(f)$, in $[(\mathrm{m/s^2})^2/\mathrm{Hz}]$, is the power spectral density of the vertical acceleration of the supporting surface.

Power spectral density $S_{ss}(f)$ is the Fourier transform of the auto-correlation function $R_{ss}(\tau)$ of the acceleration at the supporting surface $s(t)$ as mathematically described in Eqs. (2) and (3). $S_{ss}(f)$ describes how the power of a signal is distributed in the frequency domain [32].

$$S_{ss}(f) = \frac{1}{2\pi} \int_{-\infty}^{\infty} R_{ss}(\tau)\ e^{-j\,\omega\,\tau}\ d\tau, \tag{2}$$

$$R_{ss}(\tau) = \mathbf{E}[s(t)\ s(t+\tau)], \tag{3}$$

where, τ is time lag and $\omega = 2\pi f$ is the angular frequency [rad/s].

Cross spectral density $S_{sl}(f)$ is the Fourier transform of the cross-correlation $R_{sl}(\tau)$ between $s(t)$ and $l(t)$, where, $l(t)$ is the acceleration at L4. $S_{sl}(f)$ can be mathematically described in Eqs. (4) and (5) [32].

$$S_{sl}(f) = \frac{1}{2\pi} \int_{-\infty}^{\infty} R_{sl}(\tau)\ e^{-j\,\omega\,\tau}\ d\tau, \tag{4}$$

$$R_{sl}(\tau) = \mathbf{E}[s(t)\ l(t+\tau)], \tag{5}$$

Fig. 17 shows the transmissibility magnitude and its corresponding phase for the 12 test subjects, as presented by Matsomoto and Griffin [17]. In this study, the median transmissibility magnitude and phase were calculated at each frequency and elaborated in the same figure (Fig. 17) in red. As the data in Fig. 17 correspond to an even number of test subjects (12), the median can be obtained by sorting the values related to each frequency in ascending order and calculating the average of the two values in the middle. The advantage of using the median, instead of the total average, is that it does not significantly change with extreme values of some of the data (outliers).

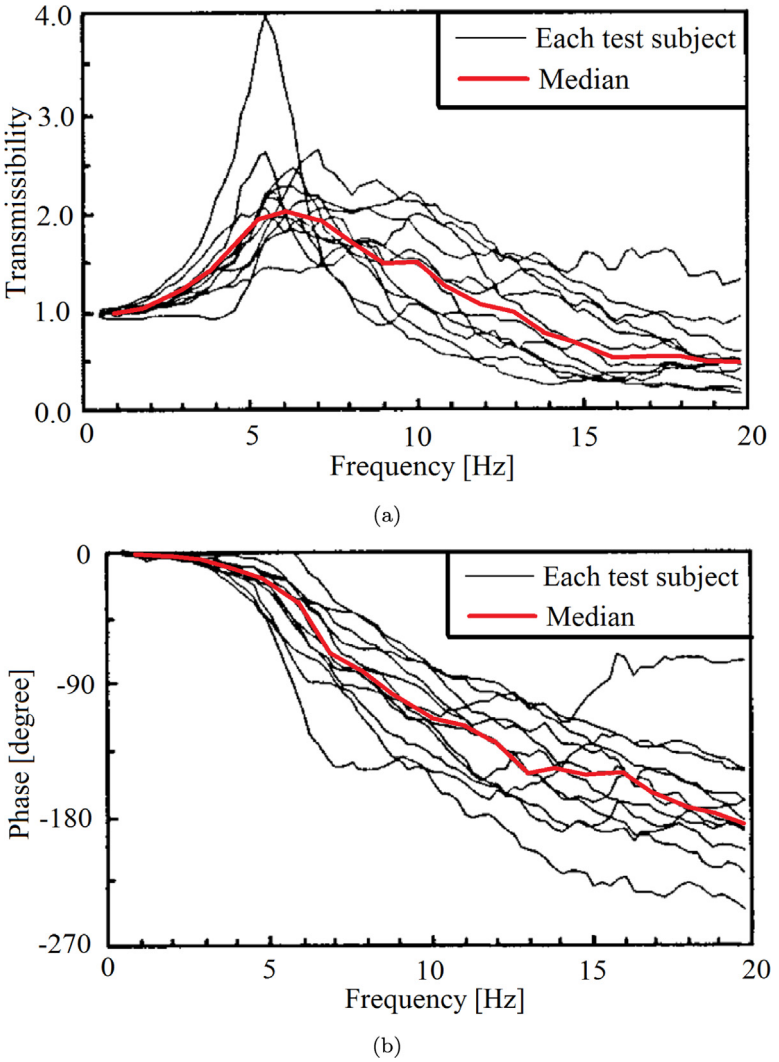

Fig. 17. (a) Transmissibility magnitude of vertical acceleration between the vibrating platform and the L4 and (b) the corresponding phase lag for 12 standing test subjects [17].

Our study utilises the above mentioned transmissibility $H_{a,a}(f)$ to calculate the acceleration at C7, instead of L4, of walking, instead of standing, individuals. These assumptions were made due to the lack of similar data related to C7 and walking individuals. If such measurements become available in the future, they can improve the proposed HSI model. Hence, the acceleration of human body mass can be calculated as follows:

- Calculate *modal* acceleration of the structure $a_{m,i}(t)$, for mode i, where m denotes the modal acceleration.
- Calculate the contribution of mode i to the physical response $a_{p,i}(t)$ using Eq. (6), where p denotes the *physical* response.

$$a_{p,i}(t) = \phi_i(v.t) \quad a_{m,i}(t), \tag{6}$$

  where, $\phi_i(v.t)$ is the mode shape amplitude of mode i at a location of a moving pedestrian walking at a constant speed v [m/s] at time t.
- The acceleration of human body mass at C7, related to mode i, $a_{h,i}(t)$, can be obtained after calculating the impulse response function $h_{a,a}(t)$, related to $H_{a,a}(f)$, as mathematically described in Eqs. (7) and (8) [32].

$$a_{h,i}(t) = \int_{-\infty}^{\infty} a_{p,i}(\tau) \; h_{a,a}(t-\tau) \; d\tau, \tag{7}$$

$$h_{a,a}(t) = \frac{1}{2\pi} \int_{-\infty}^{\infty} H_{a,a}(f) \; e^{j\,\omega\,t} \; df, \tag{8}$$

where, τ is the time step of the integration.

The impulse response function $h_{a,a}(t)$ describes the response of a system $H_{a,a}(f)$ in the time domain. Hence, there is no need to convert to the frequency domain. Eq. (7) is based on the convolution technique to find the time history response of the system $H_{a,a}(f)$ [32].

3.3. Interaction force

In this section, the calculation of the interaction force applied by a walking pedestrian on the supporting structure is described. This interaction force was assumed to be a function of the relative vertical acceleration between human body mass and the supporting structure at the point of contact between them (Fig. 15). This function ($H_{a,F}(f)$) was derived by utilising previously conducted measurements [18] of vertical acceleration of:

- human body at C7 (and three other locations on a human body not utilised in this study [18]), using inertial measurement units (IMUs), and,
- the corresponding ground reaction force, for individuals walking on an instrumented treadmill.

Fig. 18 shows test set-up for one test subject. Each TS performed at least eight minutes of walking on the treadmill as a 'warm up' before conducting the tests. Six walking tests, at the constant speed of the treadmill belt (between 0.6 m/s and 1.4 m/s), were carried out by each TS. The duration of each test was about three minutes. A detailed description of the experiments is available elsewhere [18].

In the analysis described in this section, only two minutes of data (taken at the middle of each measurement), corresponding to five TSs, were considered. Fig. 19 shows one measured time history of vertical acceleration at C7 and the corresponding ground reaction force for one TS.

A system identification process was carried out to derive a transfer function $H_{a,F}(f)$ between vertical acceleration at C7 and the corresponding ground reaction force as an input and output for $H_{a,F}(f)$, respectively. Both signals were passband filtered between 1 and 10 Hz where most of the energy was embedded and the ground reaction forces were normalised by the corresponding human body weight. To simplify the identification process, $H_{a,F}(f)$ corresponding to each test subject was assumed to be independent from the walking speed. Hence, one $H_{a,F}(f)$ was derived for each TS, using data from five walking tests, as explained below.

After initially repeating the identification process for different forms of transfer function (related to different number of poles and zeros) and assessing the curve fitting, the mathematical form described in Eq. (9) was used to derive $H_{a,F}(f)$ [33].

$$H_{a,F}(f) = \frac{P_1(j\omega)^6 + P_2(j\omega)^5 + P_3(j\omega)^4 + P_4(j\omega)^3 + P_5(j\omega)^2 + P_6(j\omega)^1 + P_7}{P_8(j\omega)^6 + P_9(j\omega)^5 + P_{10}(j\omega)^4 + P_{11}(j\omega)^3 + P_{12}(j\omega)^2 + P_{13}(j\omega)^1 + P_{14}}, \tag{9}$$

where, $P_{1,2,\ldots,14}$ are the constants to be obtained in the system identification by minimising the objective function described in Eq. (10) (based on the Non-linear Least Squares method).

$$E = \sum_{n=1}^{6}\sum_{t_i=0}^{T}(F_m(t_i,n) - F_s(t_i,n))^2, \tag{10}$$

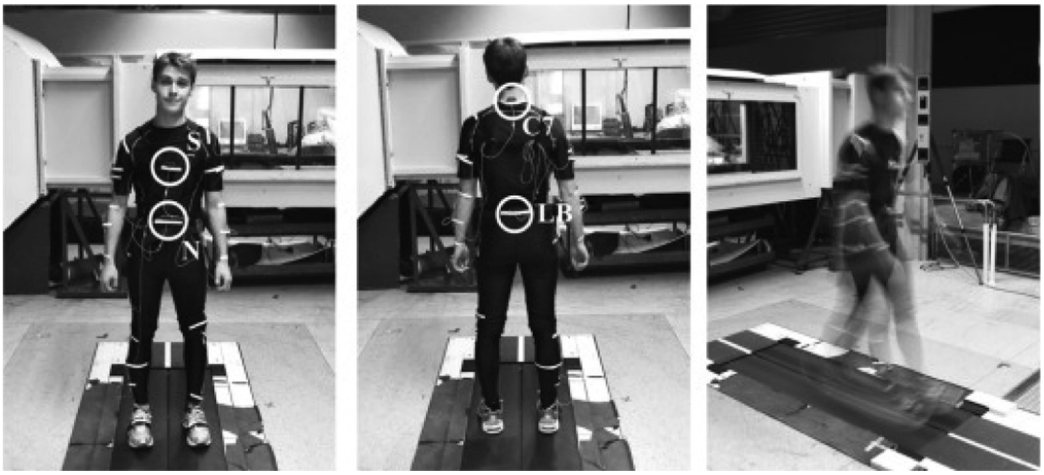

Fig. 18. Test set-up showing the location of the IMUs [18].

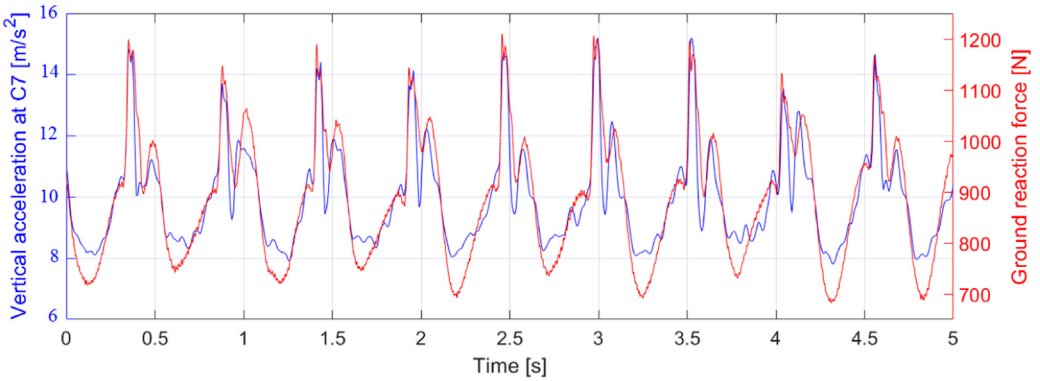

Fig. 19. Sample of vertical acceleration measured at C7 and the corresponding GRF for one test subject while walking at a pacing frequency of 1.9 Hz.

where, E is a scalar value to be minimised, n refers to each walking test conducted by a TS, t_i is time step, T is the time duration of the signal, $F_m(t_i, n)$ is the measured ground reaction force at time step t_i for walking test n. $F_s(t_i, n)$ is the simulated ground reaction force at time step t_i for walking test n, which can be obtained by simulating the discrete-time response of the transfer function $H_{a,F}(f)$ when subjected to an input signal (vertical measured acceleration of C7) [33]. The transfer functions $H_{a,F}(f)$ corresponding to the fitted parameters are shown in Fig. 20.

Interestingly, the frequency of the first peak in the magnitude of $H_{a,F}(f)$ (Fig. 20) is around 3–3.5 Hz which is within the range of frequency reported in the literature for walking individuals (2–4 Hz) [12,13,15]. The second and third peaks, at around 7–7.5 Hz and 9.5–10 Hz, respectively, could refer to possible whole-body modes of vibration for walking individuals at these frequency ranges.

To verify the applicability of the derived transfer function $H_{a,F}(f)$, one $H_{a,F}(f)$ was utilised to simulate the ground reaction force by using the acceleration measured at C7 as an input to $H_{a,F}(f)$. Fig. 21 shows that the simulated ground reaction force is quite comparable to its measured counterpart on the treadmill, especially at frequencies close to the pacing frequency. This indicates that the proposed model can work best in the case of low fundamental frequency for the floor. However, the fitting of $H_{a,F}(f)$ can be enhanced if further experimental measurements are to be conducted in the future and incorporated into the fitting process. The utilisation of $H_{a,F}(f)$ in the proposed HSI model is explained in the next subsection.

It is assumed that these transfer functions can be used to calculate both the ground reaction force related to the desire to walk on a rigid surface (from the acceleration of body mass) and the interaction force related to vibration of the supporting surface. This assumption is based on that the proposed model is related to floor structures where vibration levels are not expected to be extremely high, as for some flexible footbridges, and therefore, the transfer functions can be used for both of the above cases.

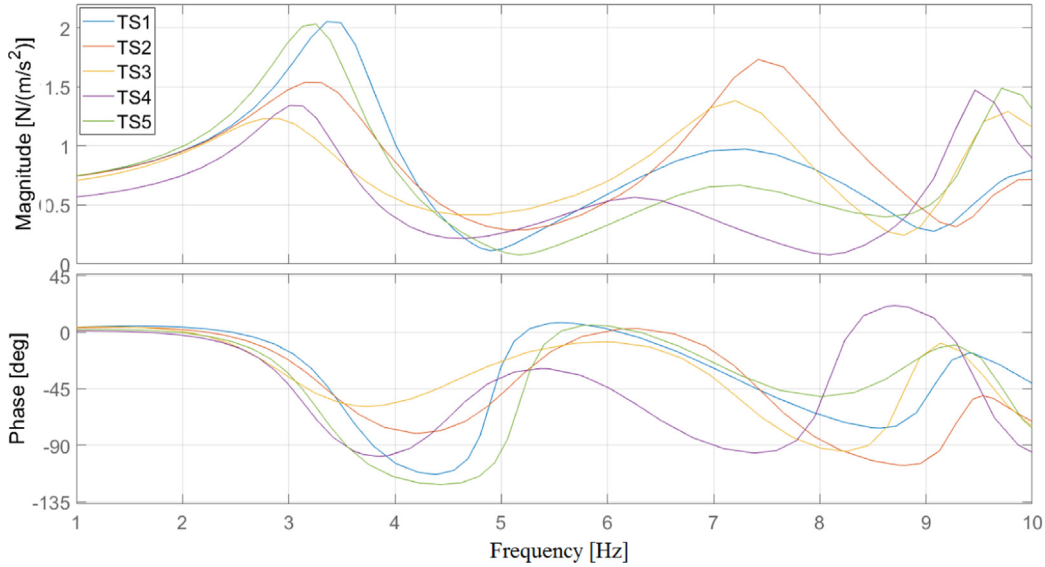

Fig. 20. The derived transfer functions ($H_{a,F}(f)$) between vertical acceleration of C7 and the corresponding ground reaction force.

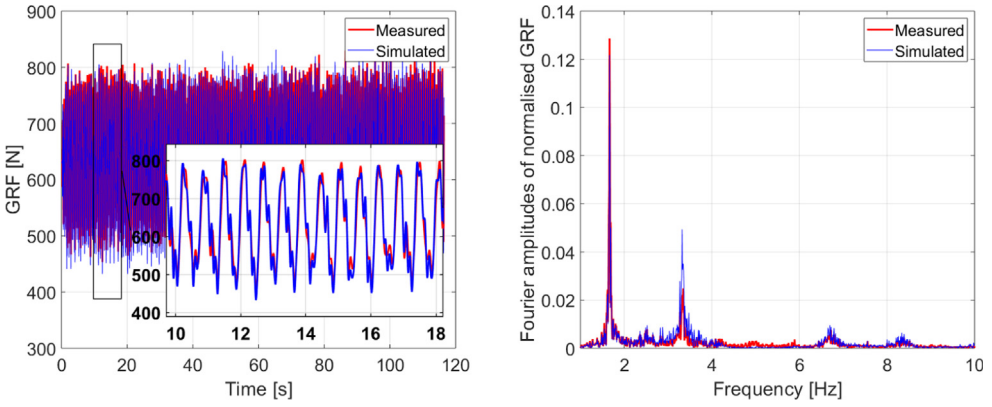

(a) Time domain. (b) Frequency domain.

Fig. 21. Measured and simulated ground reaction force using measured acceleration at C7 and one derived transfer function ($H_{a,F}(f)$).

3.4. Implementation

The two above mentioned transfer functions, $H_{a,a}(f_i)$ and $H_{a,F}(f_i)$, are to be used in each time step to simulate the interaction between the walking individual and the supporting floor. The step-by-step procedure to implement the proposed HSI methodology in the response calculation of human-induced vibration is presented below and illustrated in Fig. 22.

1. Calculate the modal acceleration response $a_{m,i}(t)$, for mode i and time step t, by solving the equation of motion, as described in Eq. (11). Note that $F_{int,i}(t-dt)$ is equal to zero at $t=0$.

$$M_i a_{m,i}(t) + C_i v_{m,i}(t) + K_i d_{m,i}(t) = GRF_r(t)\ \phi_i(v.t) + F_{int,i}(t-dt), \tag{11}$$

where, M_i, C_i and K_i are the modal mass [kg], damping coefficient [N.s/m] and stiffness [m/N] related to mode i, $\phi_i(v.t)$ is the mode shape amplitude of mode $i$at a location of moving pedestrian and $v_{m,i}(t)$ and $d_{m,i}(t)$ are the modal velocity [m/s] and modal displacement [m] responses related to mode i and time step t.

2. Calculate the contribution of mode i in the physical response at time step t ($a_{p,i}(t)$) using Eq. (6).
3. Calculate the vertical acceleration of human body mass related to mode i at time step t ($a_{h,i}(t)$), as mathematically described in Eq. (7).
4. Calculate the relative vertical acceleration $a_{rel,i}(t)$ between human body mass and the supporting structure (at the point of contact between them) related to mode i and time step t, using Eq. (12).

$$a_{rel,i}(t) = a_{h,i}(t) - a_{p,i}(t)), \tag{12}$$

5. Calculate the interaction force related to mode i and time step t ($F_{int,i}(t)$), using Eqs. (13) and (14).

$$F_{int,i}(t) = \int_{-\infty}^{\infty} a_{rel,i}(\tau)\ \ h_{a,F} \tag{13}$$

$$h_{a,F}(t) = \frac{1}{2\pi} \int_{-\infty}^{\infty} H_{a,F}(f) \tag{14}$$

here, τ is the time step of the integration.

6. Repeat steps 1–4 for all time steps until $t=T$, where T is the total duration of the simulation [s].
7. Repeat the above mentioned steps for all modes of vibration.
8. Calculate the total physical response of the floor at a location of interest ($a(t)$) using Eq. (15).

$$a(t) = \sum_{i=1}^{N} a_{m,i}(t)\ \ \phi_i(k), \tag{15}$$

where, N is the number of modes considered in the analysis and $\phi_i(k)$ is the mode shape amplitude corresponding to mode i at the node of interest (k).

4. Experimental verification

This section verifies the performance of the proposed HSI methodology using experimental acceleration response obtained from floors A and B. Simulations were carried out to calculate the corresponding vibration responses when HSI

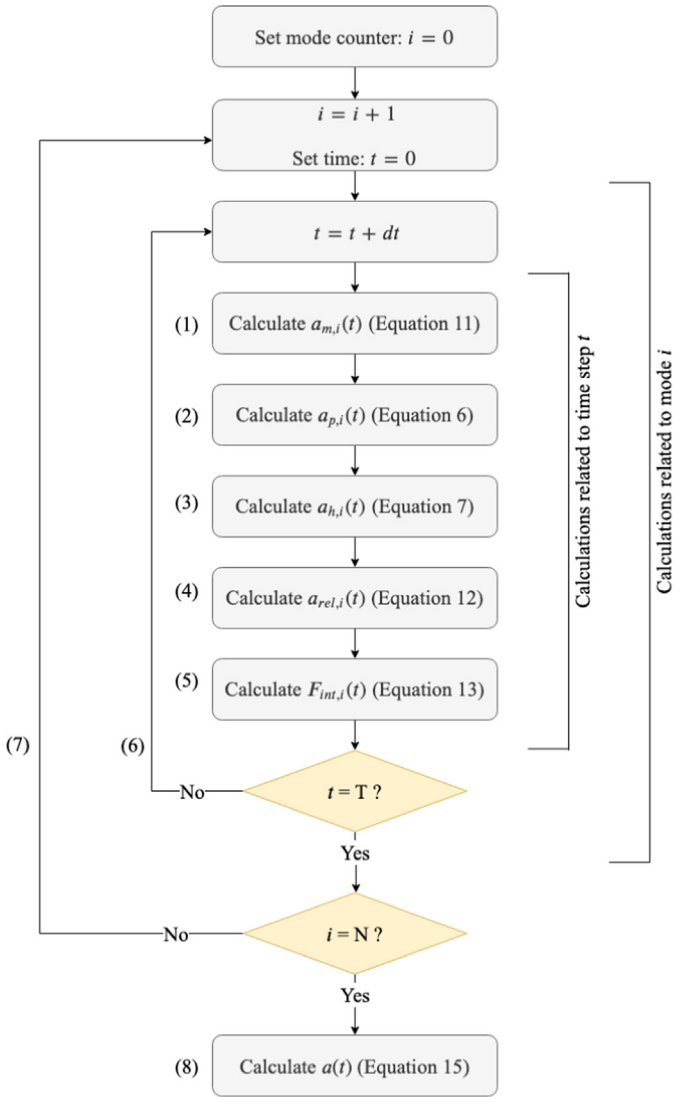

Fig. 22. Flowchart showing the steps of implementing the proposed HSI methodology.

was neglected or taken into account using the proposed methodology. The calculated responses were compared with the measurements using their maximum transient vibration value (*MTVV*), in [m/s^2], which is equal to the maximum 1 s root-mean-square (RMS). A brief discussion of the results is presented at the end of this section.

4.1. Floor A

A walking test was conducted by an individual walking along WP1 (Fig. 3). The test subject conducted a controlled walking test at a pacing frequency f_p of 1.6 Hz to achieve resonant response. The corresponding vibration response was measured at the centre of the floor (TP11 in Fig. 3). The measured response was low-pass filtered to eliminate the contribution of modes of vibration other than the first mode. This is to simplify the verification and focus on the vibration response related to the lowest mode of vibration.

The corresponding response calculation was conducted when HSI was taken into account or neglected. Previously measured ground reaction force for the same test subject while walking on an instrumented treadmill [34,3] (at the same f_p as mentioned above - 1.6 Hz) was available to be utilised for this analysis. The modal force corresponding to the first mode of vibration (Fig. 4a) was obtained by multiplying the ground reaction force of the walking pedestrian by mode shape amplitudes corresponding to WP1 (Fig. 3). The modal vibration response related to the neglected effect of HSI was calculated directly using the Newmark integration method [35]. The corresponding physical response was calculated by multiplying

the modal accelerations by the mode shape amplitude corresponding to TP11 (Fig. 3). Vibration response was also calculated using the proposed HSI methodology, as explained in Section 3.4.

The W_b weighting curve was used to obtain the weighted acceleration response ($a_w(t)$), where t is time [s] [36]. The running RMS acceleration ($a_{w,rms}(t)$) was calculated using Eq. (16).

$$a_{w,rms}(t) = \sqrt{\frac{1}{T}\int_0^T a_w^2(t)dt}, \tag{16}$$

where, T is the RMS duration (1 s) and dt is the duration of each time step [s].

The peak $a_{w,rms}(t)$ ($a_{w,rms,peak}$) is equal to the *MTVV* [m/s^2] which can be used to calculate the R factor, as described in Eq. (17).

$$R = \frac{MTVV}{0.005\ \ m/s^2}, \tag{17}$$

Fig. 23 shows the calculated and measured vibration responses. Fig. 23 shows that there is a significant overestimation of the vibration response when the influence of HSI was neglected. Implementing the proposed methodology has reduced the MTVV by around 30% and resulted in much closer vibration responses to their measured counterparts (Fig. 23).

4.2. Floor B

Walking tests were conducted by six individual test subjects, with known body mass, walking on Floor B along WP2 (Fig. 10). f_p for each test was 1.9 Hz, where its fifth integer multiple (9.5 Hz) is close to the measured fundamental frequency (9.47 Hz). The responses were measured at TP42 (Fig. 10), which is the anti-node of the first mode of vibration (Fig. 10), and low-pass filtered to eliminate the contribution of all modes of vibration other than the first mode. As no treadmill force data exists for the six test subjects, 20 measured ground reaction forces related to other people, chosen randomly, walking at the same f_p (1.9 Hz) were used in the response calculations. This was repeated when the effect of HSI was neglected and when taken into account in the response calculations. The *MTVV* corresponding to the measured and simulated responses is presented as a box plot in Fig. 24.

Fig. 24 shows that when HSI was taken into account using the proposed method, there was an average reduction in *MTVV* of about 10% compared to that when HSI was neglected. Both cases have resulted in an overestimation of the vibration responses.

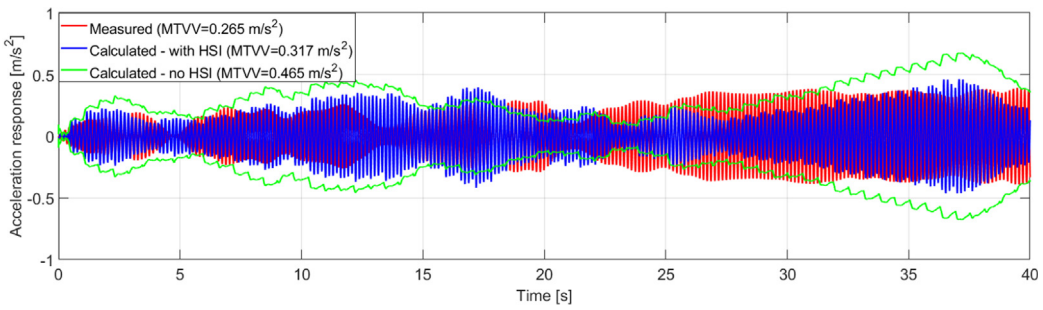

(a) Time history.

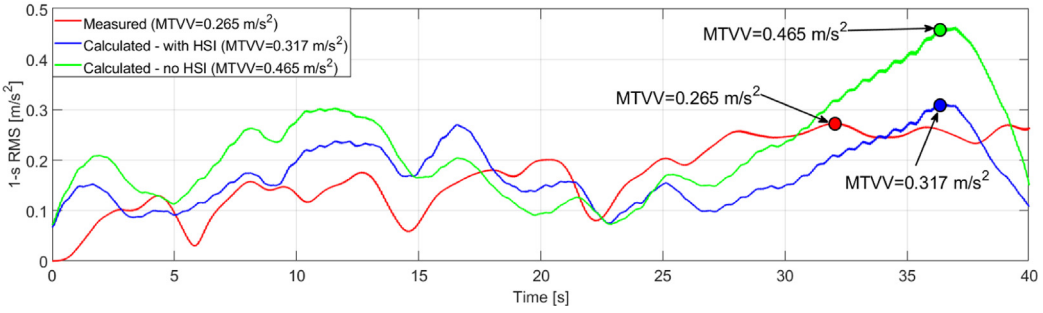

(b) RMS.

Fig. 23. (a) Vibration response related to walking along WP1 on Floor A (TP11) at f_p of 1.6 Hz (resonance) and (b) the corresponding running RMS.

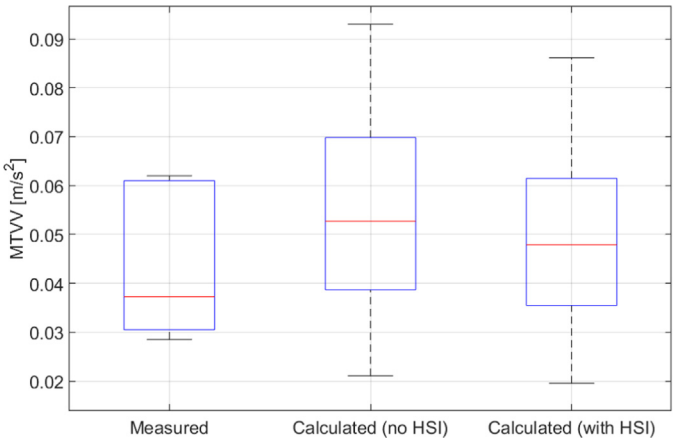

Fig. 24. *MTVV* corresponding to measured and simulated responses for six individuals walking on Floor B along WP2 (Fig. 10).

4.3. Discussion

The results presented in this section show that, in most cases, utilising the proposed HSI methodology has resulted in reduced vibration levels and more accurate prediction of vibration responses than that when HSI was neglected.

The average reduction in *MTVV* for Floor B when HSI was taken into account (10%, as shown in Fig. 24) was less than that for Floor A (30%, as shown in Fig. 4a). Interestingly, the maximum reduction in *MTVV* for each floor is comparable to the reduction of its FRF magnitude at the fundamental frequency when occupied by single or multiple pedestrians (Table 1) despite the differences between the two concepts.

The results presented in this section show that utilising the proposed HSI methodology has resulted in an improved estimation of human-induced vibration levels for floors. This is confirmed by the tests conducted on the two floors discussed in this paper.

5. Parametric study

In this section, a parametric study was conducted to examine how the dynamic properties of a floor modelled as SDOF oscillator (natural frequency, modal mass and modal damping ratio) affect the influence of HSI on the vibration responses. This was achieved by calculating vibration response, corresponding to the lowest mode of vibration, related to an imaginary scenario of a pedestrian walking on Floor A and across WP1 (Fig. 3). For each case explained below, the *MTVV* was calculated when HSI was neglected and when it was taken into account using the proposed HSI method, and the reduction in *MTVV* was utilised for comparison, as explained below.

5.1. Natural frequency effects

The influence of the natural frequency on HSI can be examined by using the same modal mass (3,019 kg) and modal damping ratio (0.5%) as measured for Floor A (Fig. 4a) but with different natural frequencies. The choice of natural frequencies is explained below.

Six ground reaction forces, measured previously using an instrumented treadmill [34,3], were chosen for random individuals walking at different f_p (1.6, 1.75, 1.85, 1.9, 2.1 and 2.3 Hz). As the influence of HSI on vibration responses is relatively high in the case of a resonant response, it was decided to make the natural frequency equal to an integer multiple of f_p but below 10 Hz. Table 2 shows the natural frequencies used with each f_p. The reduction in *MTVV* was calculated for each pair of f_p and a corresponding natural frequency (Table 2), and the results are shown in Fig. 25a.

Table 2
f_p and the corresponding natural frequencies used in the parametric study.

f_p [Hz]	Corresponding natural frequencies [Hz]
1.60	1.60, 3.20, 4.80, 6.40, 8.00 and 9.60
1.75	1.75, 3.5, 5.25, 7.0 and 8.75
1.85	1.85, 3.7, 5.85, 7.4 and 9.25
1.90	1.90, 3.80, 5.70, 7.60 and 9.50
2.10	2.10, 4.20, 6.30 and 8.40
2.30	2.30, 4.60, 6.90 and 9.20

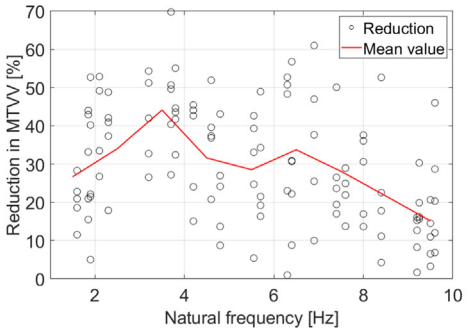

(a) Reduction in $MTVV$ for different natural frequencies of the empty floor.

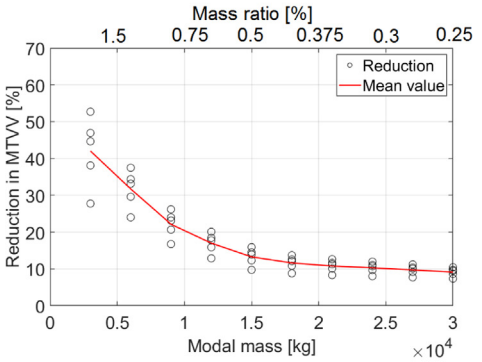

(b) Reduction in $MTVV$ for different modal masses and mass ratios of the empty floor.

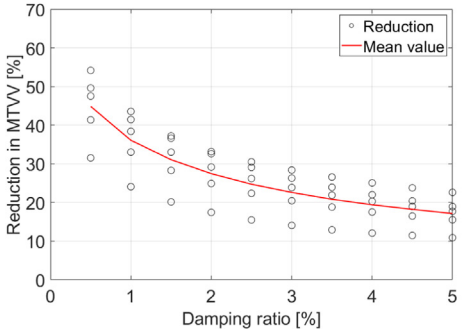

(c) Reduction in $MTVV$ for different modal damping ratios of the empty floor.

Fig. 25. The influence of (a) natural frequency, (b) modal mass and (c) modal damping ratio of a floor on the reduction in *MTVV* when HSI was taken into account.

5.2. Modal mass and modal damping ratio effects

The influence of the modal mass on HSI was examined by using the measured fundamental frequency (6.36 Hz) and modal damping ratio of the first mode of vibration (0.5%) (Fig. 4a) but with varying value of modal mass between 3,000 kg and 30,000 kg. The range of the chosen modal mass corresponds to a mass ratio, the ratio between human body mass and the modal mass for the lowest mode of vibration, between 2.5% and 0.25%. The corresponding reduction of *MTVV* is shown in Fig. 25b.

Similarly, the influence of the modal damping ratio on HSI was examined by using the measured fundamental frequency (6.36 Hz) and modal mass (3,019 kg) of the first mode (Fig. 4a) but with varying value of modal damping ratio between 0.5% and 5%. The corresponding reduction of *MTVV* is shown in Fig. 25c.

5.3. Discussion

Fig. 25a shows that maximum reduction in *MTVV*, related to utilising the proposed HSI model, appears at 3–4 Hz and around 7 Hz. This is comparable with the peaks of $H_{a,F}(f)$ magnitude as shown in Fig. 20. Furthermore, higher modal mass (i.e. lower mass ratio) and/or damping ratio has resulted in less reduction in *MTVV* (Fig. 25b and Fig. 25c).

The results presented in Fig. 25 can assist designers in estimating the range of reduction in *MTVV* for a floor. For example, Fig. 25 can be used to estimate the reduction in *MTVV* for Floor B when only the first mode of vibration is considered (Fig. 11a) as follows:

- An initial reduction in *MTVV* can be picked from Fig. 25a as around 18% (average reduction in *MTVV* corresponding to a fundamental frequency of 9.47 Hz)
- As the data presented in Fig. 25a corresponds to a modal mass and damping ratio of 22,478 kg and 0.4%, respectively (Fig. 11a), interpolation should be made (using Fig. 25b and Fig. 25c) to adjust the initial reduction in *MTVV* accordingly. This will result in an around 5% reduction in *MTVV*.

This estimated small reduction in *MTVV* related to Floor B is consistent with the relatively small reduction of *MTVV* for the simulations conducted for the same floor, as shown in Fig. 24.

6. Conclusions

This work quantifies the effect of walking pedestrians on the FRF magnitude for two floors and presents a methodology that takes HSI into account in the response calculation of human-induced vibration of floors. Experimental measurements of two floors show the potential for a significant reduction in their FRF magnitude when they are occupied by walking pedestrians. The amount of this reduction is apparently affected by the natural frequency and modal mass.

In contrast to other HSI models available in the literature, the proposed model takes into account human dynamics using two transfer functions and over a range of frequencies (1–10 Hz) rather than using MSD or IP models. The advantage of this modelling approach is that it takes into account the complexity of human whole-body dynamics using simple experimentally-based transfer functions that can be used to calculate:

- Acceleration of the human body due to structural acceleration of the supporting structure, and
- The corresponding interaction force acting on the structure.

The performance of the proposed model was verified using experimental measurements of individuals walking on two floors. Consistent results were observed between measured and simulated responses. The responses calculated using the proposed model were lower than those calculated when HSI was neglected but still higher than their measured counterparts. This implies that the proposed model can be utilised to predict reliable and conservative estimation of the vibration levels.

The derivation of the two transfer functions, related to the proposed HSI model, was not based on a specific type of floor as they were obtained from measurements conducted, in previous studies, for people walking on an instrumented treadmill or standing on a vibrating platform. Hence, it is believed that the proposed method can be used for any type of floor. However, this method should be used only for floor modes of vibrations with a natural frequency of less than 10 Hz (i.e. low-frequency floors). This is so because the proposed HSI methodology was derived for this range of frequencies due to inaccuracies related to higher frequencies for C7 vertical acceleration measurements caused by skin movement artefacts during walking. Furthermore, it is expected that the methodology works best for floors with relatively low fundamental frequencies where the fitting of the transfer functions appears to be better than that close to 10 Hz. Furthermore, this study utilises a limited amount of experimental data related to a small number of test subjects to derive the transfer functions. Further measurements related to higher number of test subjects walking on a vibrating surface can be conducted in the future to enhance the fitting of the derived transfer functions and ensure the statistical reliability of the proposed HSI model.

CRediT authorship contribution statement

Ahmed Mohammed: Methodology, Software, Validation, Formal analysis, Investigation, Data curation, Writing - original draft, Visualization. **Aleksandar Pavic:** Supervision, Conceptualization, Resources, Writing - review & editing, Supervision, Project administration.

Declaration of Competing Interest

Data Statement The core data used to derive the model proposed in this paper were generated in a separate research project (https://www.sciencedirect.com/science/article/pii/S0022460X16301031) and provided to us by Prof James Brownjohn of Vibration Engineering Section, University of Exeter. Therefore, they do not belong to the authors and they cannot share

them publicly. The rest of the data are not available due to ethical concerns, as participants did not consent to the sharing of their data, and as such the data supporting this publication are not available.

Acknowledgments

The authors acknowledge the financial support, which came from the University of Exeter doctoral scholarship for Dr Mohammed and the UK Engineering and Physical Sciences Research Council (EPSRC) for the following research grants:

- Platform Grant EP/G061130/2 (Dynamic performance of large civil engineering structures: an integrated approach to management, design and assessment), and
- Frontier Engineering Grant EP/K03877X/1 (Modelling complex and partially identified engineering problems: Application to the individualised multi-scale simulation of the musculoskeletal system).

The authors are grateful to WSP, LV= and Summerfield Developments for their assistance and for facilitating the experimental work. The authors are also thankful to Prof James Brownjohn for providing experimental data regarding human walking tests on an instrumented treadmill.

References

[1] P.K. Nag, Office Buildings: Health, Safety and Environment, Springer, 2018.
[2] W. Ferdous, Y. Bai, T.D. Ngo, A. Manalo, P. Mendis, New advancements, challenges and opportunities of multi-storey modular buildings – a state-of-the-art review, Eng. Struct. 183 (2019) 883–893, https://doi.org/10.1016/j.engstruct.2019.01.061.
[3] J.M.W. Brownjohn, V. Racic, J. Chen, Universal response spectrum procedure for predicting walking-induced floor vibration, Mech. Syst. Signal Process. (2015) 1–15, https://doi.org/10.1016/j.ymssp.2015.09.010, URL: http://linkinghub.elsevier.com/retrieve/pii/S0888327015004057.
[4] A. Pavic, M.R. Willford, Vibration Serviceability of Post-tensioned Concrete Floors – CSTR43 App G, Technical Report, Slough, UK, 2005..
[5] M.R. Willford, P. Young, A Design Guide for Footfall Induced Vibration of Structures – CCIP-016, The Concrete Centre, Slough, 2006.
[6] M. Feldmann, C. Heinemeyer, Human Induced Vibration of Steel Structures - Vibration Design of Floors: Guideline, Research for coal and steel, 2007. URL: http://www.stb.rwth-aachen.de/projekte/2007/HIVOSS/download.php..
[7] A.L. Smith, S.J. Hicks, P.J. Devine, Design of Floors for Vibration – A New Approach SCI P354, Revised Ed, volume SCI P354, The Steel Construction Institute, 2009..
[8] D.A. Fanella, M. Mota, Design Guide for Vibrations of Reinforced Concrete Floor Systems, first ed., CRSI, 2014..
[9] T.M. Murray, D.E. Allen, E.E. Ungar, D.B. Davis, Vibrations of Steel-Framed Structural Systems Due to Human Activity: AISC DG11 (Technical Report), second ed., American Institute of Steel Construction (AISC), 2016.
[10] M. Bocian, J.H.G. Macdonald, J.F. Burn, Biomechanically inspired modeling of pedestrian-induced vertical self-excited forces, J. Bridge Eng. 18 (2013) 1336–1346, https://doi.org/10.1061/(ASCE)BE.1943-5592.0000490.
[11] J.W. Qin, S.S. Law, Q.S. Yang, N. Yang, Pedestrian-bridge dynamic interaction, including human participation, J. Sound Vib. 332 (2013) 1107–1124, https://doi.org/10.1016/j.jsv.2012.09.021.
[12] C. Caprani, E. Ahmadi, Formulation of human-structure interaction system models for vertical vibration, J. Sound Vib. 377 (2016) 346–367, https://doi.org/10.1016/j.jsv.2016.05.015.
[13] M. Toso, H. Gomes, F. da Silva, R. Pimentel, Experimentally fitted biodynamic models for pedestrian-structure interaction in walking situations, Mech. Syst. Signal Process. (2015) 1–17, https://doi.org/10.1016/j.ymssp.2015.10.029, URL: http://linkinghub.elsevier.com/retrieve/pii/S0888327015004896.
[14] K. Van Nimmen, G. Lombaert, G. De Roeck, P. Van den Broeck, The impact of vertical human-structure interaction on the response of footbridges to pedestrian excitation, J. Sound Vib. 402 (2017) 104–121, https://doi.org/10.1016/j.jsv.2017.05.017.
[15] E. Shahabpoor, A. Pavic, V. Racic, Identification of mass-spring-damper model of walking humans, Structures 5 (2016) 233–246, https://doi.org/10.1016/j.istruc.2015.12.001, URL:/http://www.sciencedirect.com/science/article/pii/S2352012415001332 http://linkinghub.elsevier.com/retrieve/pii/S2352012415001332.
[16] E. Shahabpoor, A. Pavic, V. Racic, Interaction between walking humans and structures in vertical direction: A literature review, Shock Vib. 2016 (2016) 12–17, https://doi.org/10.1155/2016/3430285.
[17] Y. Matsumoto, M.J. Griffin, Dynamic response of the standing human body exposed to vertical vibration: Influence on posture and vibration, J. Sound Vib. 212 (1998) 85–107, https://doi.org/10.1006/jsvi.1997.1376, URL: http://linkinghub.elsevier.com/retrieve/pii/S0022460X97913766.
[18] M. Bocian, J.M.W. Brownjohn, V. Racic, D. Hester, A. Quattrone, R. Monnickendam, A framework for experimental determination of localised vertical pedestrian forces on full-scale structures using wireless attitude and heading reference systems, J. Sound Vib. 376 (2016) 217–243, https://doi.org/10.1016/j.jsv.2016.05.010.
[19] S. Zivanovic, Benchmark footbridge for vibration serviceability assessment under the vertical component of pedestrian load, J. Struct. Eng. 138 (2012) 1193–1202, https://doi.org/10.1061/(ASCE)ST.1943-541X.0000571.
[20] E. Ahmadi, C. Caprani, S. Živanović, A. Heidarpour, Vertical ground reaction forces on rigid and vibrating surfaces for vibration serviceability assessment of structures, Eng. Struct. 172 (2018) 723–738, https://doi.org/10.1016/j.engstruct.2018.06.059.
[21] APS Dynamics Inc., Instruction manual, ELECTRO-SEIS, Model 400 Shaker, APS Dynamics Inc, 2013..
[22] APS Dynamics Inc., Instruction manual, ELECTRO-SEIS, Model 113 Shaker, APS Dynamics Inc, 1996..
[23] D.J. Ewins, Modal Testing: Theory, Practice and Application, Research Studies Press Ltd., Baldock, Hertfordshire, England, 2000.
[24] Vibrant Technology Inc., ME'Scope VES - VT560 Visual SDM Pro, 2018..
[25] M. Geradin, D.J. Rixen, Mechanical Vibrations: Theory and Application to Structural Dynamics, third ed., John Wiley and Sons, 2015..
[26] E.J. Hudson, P. Reynolds, Design and Construction of a Reconfigurable Pedestrian Structure, Exp. Tech. (2016), https://doi.org/10.1007/s40799-016-0144-3, URL: http://link.springer.com/10.1007/s40799-016-0144-3.
[27] A.S. Mohammed, A. Pavic, Effect of walking people on dynamic properties of floors, Proc. Eng. 199 (2017) 2856–2863, https://doi.org/10.1016/j.proeng.2017.09.561.
[28] S. Zivanovic, I. Diaz, A. Pavic, Influence of walking and standing crowds on structural dynamic performance, in: 27th International Modal Analysis Conference (IMACXXVII), 2009.
[29] E. Shahabpoor, A. Pavic, Estimation of vertical walking ground reaction force in real-life environments using single IMU sensor, J. Biomech. 79 (2018) 181–190, https://doi.org/10.1016/j.jbiomech.2018.08.015.
[30] E. Shahabpoor, A. Pavic, V. Racic, Structural vibration serviceability: new design framework featuring human-structure interaction, Eng. Struct. 136 (2017) 295–311, https://doi.org/10.1016/j.engstruct.2017.01.030.
[31] M. Griffin, Handbook of Human Vibration, Academic Press, London, 1990.

[32] K.G. McConnell, P.S. Varoto, Vibration Testing: Theory and Practice, second ed., John Wiley and Sons Inc, 2008, URL:http://books.google.com/books?hl=en&lr=&id=tv8MiE2By74C&pgis=1..
[33] K. Gopalan, Introduction to Signals and Systems Analysis, Cengage Learning Inc, Belmont, CA, United States, 2012.
[34] V. Racic, J.M.W. Brownjohn, Stochastic model of near-periodic vertical loads due to humans walking, Adv. Eng. Inf. 25 (2011) 259–275, https://doi.org/10.1016/j.aei.2010.07.004, URL: http://linkinghub.elsevier.com/retrieve/pii/S1474034610000716.
[35] M. Paz, W. Leigh, Structural Dynamics, Springer, US, Boston, MA, 2004. URL: http://link.springer.com/10.1007/978-1-4615-0481-8.https://doi.org/10.1007/978-1-4615-0481-8..
[36] BS 6841-1987, BS 6841-1987 Guide to measurement and evaluation of human exposure to whole-body mechanical vibration and repeated shock, 1987..